Cellular/Molecular

Regulation of Neurite Growth by Spontaneous Ca^{2+} Oscillations in Astrocytes

Kazunori Kanemaru,[1] Yohei Okubo,[1] Kenzo Hirose,[2] and Masamitsu Iino[1]

[1]Department of Pharmacology, Graduate School of Medicine, The University of Tokyo, Bunkyo-ku, Tokyo 113-0033, Japan, and [2]Department of Cell Physiology, Nagoya University Graduate School of Medicine, Nagoya 466-8550, Japan

Astrocytes play a pivotal role in the regulation of neurite growth, but the intracellular signaling mechanism in astrocytes that mediates this regulation remains unclarified. We studied the relationship between spontaneous Ca^{2+} oscillations in astrocytes and the astrocyte-mediated neurite growth. We generated Ca^{2+} signal-deficient astrocytes in which spontaneous Ca^{2+} oscillations were abolished by a chronic inhibition of IP_3 signaling. When hippocampal neurons were cultured on a monolayer of Ca^{2+} signal-deficient astrocytes, the growth of dendrites and axons was inhibited. Time-lapse imaging of the advancement of axonal growth cones indicated the involvement of membrane-bound molecules for this inhibition. Among six candidate membrane-bound molecules that may modulate neuronal growth, N-cadherin was downregulated in Ca^{2+} signal-deficient astrocytes. Although a blocking antibody to N-cadherin suppressed the axonal growth on control astrocytes, extrinsic N-cadherin expression rescued the suppressed axonal growth on Ca^{2+} signal-deficient astrocytes. These findings suggest that spontaneous Ca^{2+} oscillations regulate the astrocytic function to promote neurite growth by maintaining the expression of specific growth-enhancing proteins on their surface, and that N-cadherin is one of such molecules.

Key words: **spontaneous calcium oscillation; neuron-glia interaction; neurite growth; inositol 1,4,5-trisphosphate; astrocyte; N-cadherin**

Introduction

Astrocytes, the predominant type of glial cells in the CNS, regulate neuronal development not only as the supporting scaffold for neuronal structures but also as the active provider of various signaling molecules to neurons (Ullian et al., 2001; Araujo and Tear, 2003; Hama et al., 2004). One of the most important functions of astrocytes is the regulation of neurite growth. Astrocytes promote neurite growth by providing various diffusible and nondiffusible proteins (Tomaselli et al., 1988; Powell et al., 1997; Crone and Lee, 2002; Araujo and Tear, 2003). In contrast, astrocytes around injury sites of the brain change into reactive astrocytes that overexpress growth-inhibitory extracellular matrix (ECM) proteins and suppress the extension of regenerating axons (Silver and Miller, 2004). Moreover, astrocytes lose their function to promote neurite growth with age (Bahr et al., 1995). Thus, astrocytes change their properties with regard to the promotion of neurite growth depending on their environments or on the developmental stage. However, the underlying mechanism that controls this property remains unclarified.

The development of Ca^{2+} imaging techniques led to the finding that astrocytes show dynamic intracellular Ca^{2+} signals (Verkhratsky et al., 1998; Parri et al., 2001; Aguado et al., 2002; Nett et al., 2002; Koizumi et al., 2003; Hirase et al., 2004; Wang et al., 2006). Astrocytes show not only Ca^{2+} transients evoked by neurotransmitters but also ongoing spontaneous Ca^{2+} oscillations in the absence of neuronal activities (Verkhratsky et al., 1998; Nett et al., 2002; Koizumi et al., 2003; Hirase et al., 2004). Although it is a remarkable feature for nonexcitable cells to generate spontaneous Ca^{2+} oscillations, their physiological significance remains unclear. Interestingly, it was reported that spontaneous Ca^{2+} oscillations became less frequent with age (Parri et al., 2001) and were lost in reactive astrocytes (Aguado et al., 2002). It is therefore probable that spontaneous Ca^{2+} oscillations are involved in the function of astrocytes to promote neurite growth. However, the lack of suitable methods to specifically and chronically inhibit astrocytic Ca^{2+} signals prevented us from clarifying this possibility.

To address this issue, we suppressed astrocytic Ca^{2+} signals chronically by stable expression of IP_3 5-phosphatase (5ppase), an enzyme that specifically hydrolyzes IP_3 (Laxminarayan et al., 1994; Hirose et al., 1999; Okubo et al., 2001, 2004; Furutani et al., 2006; Suh et al., 2006). In the neurons cultured on these astrocytes, neurite growth in terms of dendritic growth and growth cone advancement was significantly suppressed. Remarkably, using time-lapse imaging of growth cone advancement, we found the involvement of nondiffusible molecules on the extracellular surface of astrocytes in the inhibition of neurite growth. Moreover, we found the decreased expression level of N-cadherin, a potent enhancer of neurite growth, in Ca^{2+} signal-deficient astrocytes and its significant responsibility for the inhibition of neurite growth. These findings indicate an essential role of astrocytic spontaneous Ca^{2+} oscillations in neurite growth and suggest a new Ca^{2+} oscillation-dependent regulation of N-cadherin expression in astrocytes.

Received May 18, 2007; revised June 25, 2007; accepted July 8, 2007.

This work was supported by grants from the Ministry of Education, Culture, Sports, Science and Technology, Japan and from the Takeda Science Foundation. We thank Y. Kawashima, Y. Yoshizawa, Y. Sato, Y. Sasagawa, T. Yamazawa, A. Mizushima, and M. Fujii for technical assistance.

Correspondence should be addressed to Masamitsu Iino at the above address. E-mail: iino@m.u-tokyo.ac.jp.

DOI:10.1523/JNEUROSCI.2276-07.2007

 0270-6474/07/278957-10$15.00/0

Materials and Methods

Viral vectors. We subcloned a retroviral vector (pMX) (Miyakawa et al., 2001) encoding cDNAs of rat wild-type 5ppase (Hirose et al., 1999) or its mutants [R343A (Okubo et al., 2001) and R343A/R350A] and internal ribosomal entry site 2 (IRES2)-Discosoma red 2 (DsRed2; Clontech, Palo Alto, CA) as a transfection marker. Mutations were introduced by PCR using mutated primers. N-cadherin-cyan fluorescent protein (Teng et al., 2005) [kindly provided by Drs. Y. Tanaka, N. Hirokawa (The University of Tokyo, Tokyo, Japan) and M. Takeichi (Kyoto University, Kyoto, Japan)] was also subcloned into the retroviral vector. Retroviral particles were produced as described previously (Miyakawa et al., 2001). Briefly, pMX (24 μg) and the vesicular somatitis virus G glycoprotein (VSV-G)-encoding vector (pVSVG, 4 μg; Clontech) were cotransfected into a pantropic packaging cell line, GP293 (Clontech), using Lipofectamine 2000 (Invitrogen, Carlsbad, CA). Two days later, retroviral particles were collected from the medium and used for infection after concentration by centrifugation (8000 × *g* for 16 h). Lentiviral vectors harboring the construct of DsRedExpress (Invitrogen) or Inverse Pericam2 (to lower pH sensitivity, Q69M mutation was introduced into circularly permuted yellow fluorescent protein in Inverse Pericam) (Nagai et al., 2001) were produced by replacing the cDNA of enhanced green fluorescent protein (GFP) in FUGW (Lois et al., 2002) [together with pVSV-G and pΔ8.9; kindly provided by Drs. C. Lois (Massachusetts Institute of Technology, Cambridge, MA) and D. Baltimore (Caltech, Pasadena, CA)]. Lentiviral particles were produced by the same procedure described above except that the lentiviral vector (15 μg), pVSV-G (4 μg), and pΔ8.9 (8 μg) were cotransfected into 293FT cells (Invitrogen).

Cell cultures and virus infection. Astrocytes and neurons were prepared from the hippocampus of Sprague Dawley rat fetuses [embryonic day 18 (E18) to E19] using the same procedure described previously (Goslin et al., 1998), confirming with guidelines established by the Animal Welfare Committee of the University of Tokyo. Briefly, the minced hippocampus was treated with 2.5% trypsin (Invitrogen) and 0.1% DNase I (Sigma, St. Louis, MO) in Ca^{2+}/Mg^{2+}-free PBS for 5 min at room temperature (RT) (22–24°C). The cells were washed with DMEM (Sigma) supplemented with 10% fetal calf serum, penicillin (100 U/ml), streptomycin (100 U/ml), and 2 mM L-glutamine (Sigma) and dissociated by trituration with a fire-polished Pasteur pipette in Ca^{2+}/Mg^{2+}-free PBS containing 0.05% DNase I and 0.03% trypsin inhibitor (Sigma).

To obtain astrocytes, the dissociated cells were plated at a high density (4.0–5.0 × 10^5 cells/cm^2) on a collagen type I-coated dish (IWAKI, Tokyo, Japan) and cultured at 37°C in DMEM supplemented as described above. After replating three times, we obtained a monolayer of astrocytes [>95% of cells expressed an astrocyte marker, glial fibrillary acidic protein (GFAP)]. For the production of astrocytes stably expressing 5ppase, its mutants or DsRed2 only, the retroviruses were added to the culture medium so that 60–95% of astrocytes were transduced. Additional replating, at least two times, was performed for the following experiments. These astrocytes replated five to seven times in total formed normal monolayers. We confirmed that cell viability of 5ppase-expressing and thapsigargin-pretreated (see Fig. 1) astrocytes was retained even after culturing for 1 month and 36 h, respectively, with trypan blue staining (data not shown). Cocultured neurons were viable for >30 d on the monolayer of astrocytes with and without infection of each virus.

For the astrocyte–neuron coculture, a confluent monolayer of the astrocytes was prepared by plating transduced astrocytes on a glass-bottomed dish (Greiner Bio-One, Frick-enhausen, Germany) coated with collagen type-I (IFP, Yamagata, Japan) and poly-L-lysine (Sigma) and then incubated for ~16 h. The dissociated cells described above were plated on the astrocyte monolayer at a low density (1.0 × 10^3 cells/cm^2) to avoid the contamination of uninfected glial cells. The cells were cultured in Neurobasal-A (Invitrogen) with B-27 supplement (Invitrogen), penicillin (100 U/ml), streptomycin (100 U/ml), and 2 mM L-glutamine. The medium was changed every 3 d by replacing one-half of the old medium with a fresh one. For GFP expression in cocultured neurons, lentiviral particles (FUGW; see above) were added to the culture medium so that >90% of hippocampal neurons were infected. After culturing for 24 h, the medium was totally replaced with a flesh medium. Although some astrocytes were also infected, the GFP expression level in these cells was negligibly lower than in neurons 5–7 d after infection.

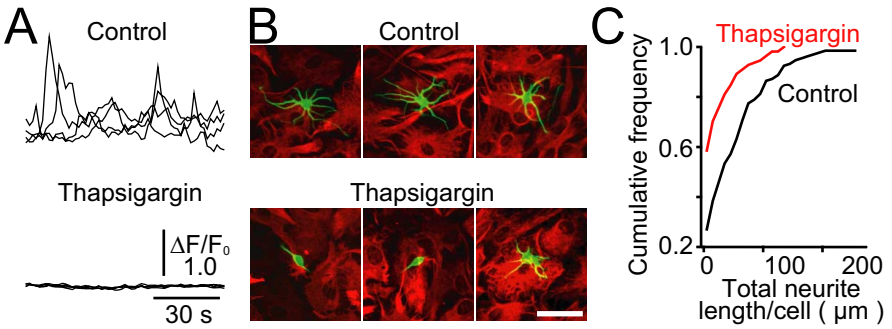

Figure 1. Suppression of neurite growth on astrocytes in which Ca^{2+} signals were pharmacologically inhibited. ***A***, Inhibition of spontaneous Ca^{2+} oscillations in astrocytes by thapsigargin pretreatment. Astrocyte monolayers were treated with thapsigargin (1 μM) for 15 min, and then thapsigargin was washed away. Spontaneous Ca^{2+} oscillations in astrocytes with or without thapsigargin pretreatment were measured with fluo-4. Four representative traces of normalized fluorescence intensity ($\Delta F/F_0$) are shown. The thapsigargin-treated astrocytes remained Ca^{2+} signal-deficient for at least 3 d after the withdrawal of the drug. ***B***, Representative images of immunostained neurons (class III β-tubulin; green) cultured for 36 h on astrocytes (GFAP; red). Scale bar, 50 μm. ***C***, Total neurite length per cell is shown as cumulative histograms. $n = 133$ for control, $n = 111$ for thapsigargin. The statistical significance ($p < 0.001$) between two cumulative histograms was confirmed by the Kolmogorov–Smirnov test.

Imaging. For Ca^{2+} imaging, astrocytes on a glass-bottomed dish coated with collagen type-I and poly-L-lysine were loaded with 5 μM fluo-4 AM (Invitrogen) or fura-2 AM (Dojindo, Kumamoto, Japan) for 45–60 min at RT. Spontaneous Ca^{2+} oscillations in fluo-4-loaded astrocytes were imaged using IX81-ZDC inverted microscope (Olympus, Tokyo, Japan) equipped with an electron multiplying CCD camera (C9100–02; Hamamatsu, Shizuoka, Japan), an electric XY-stage (MD-WELL96100T-META; Molecular Devices, Sunnyvale, CA), and a xenon lamp [excitation, ~480 nm; emission, <515 nm; objective lens, 20×; numerical aperture (NA) 0.5; UPlanFL N, Olympus]. The fluorescence images of fura-2-loaded astrocytes were captured using an Olympus IX70 inverted microscope equipped with a cooled CCD camera (Quantix A97G6000; Photometrics, Tucson, AZ) and a polychromatic illumination system (Polychrome II; TILL Photonics, Munich, Germany) with excitation at 345 and 380 nm (emission, <510 nm; objective lens, 40×; NA 0.8; LUMPlanFl, Olympus). The intracellular Ca^{2+} concentration in fura-2-loaded cells was calibrated as reported previously (Miyakawa et al., 2001).

For the time-lapse imaging of growth cone movement, growth cones of GFP-expressing neurons cultured on the astrocyte monolayer within the culture medium (see above) without phenol red were imaged using the Olympus IX81-ZDC system (excitation, ~480 nm, emission, <510 nm for GFP; excitation, ~520 nm, emission, ~590 nm for DsRed2) at 37°C in 5% CO_2. We analyzed advancing axonal growth cones with an obvious palm-like morphology and a high motility. Growth cones that showed successive retractions were excluded from analysis. For the evaluation of N-cadherin function in growth cone advancement (see Fig. 7*E*), function-blocking antibody to N-cadherin (clone GC-4; 10 μg/ml; Sigma) or control antibody (anti-FLAG M2, 10 μg/ml; Sigma) was added to the culture medium 3 h before imaging.

For the simultaneous imaging of growth cone advancement and astrocytic Ca^{2+} signals, astrocytes were infected with lentiviruses harboring

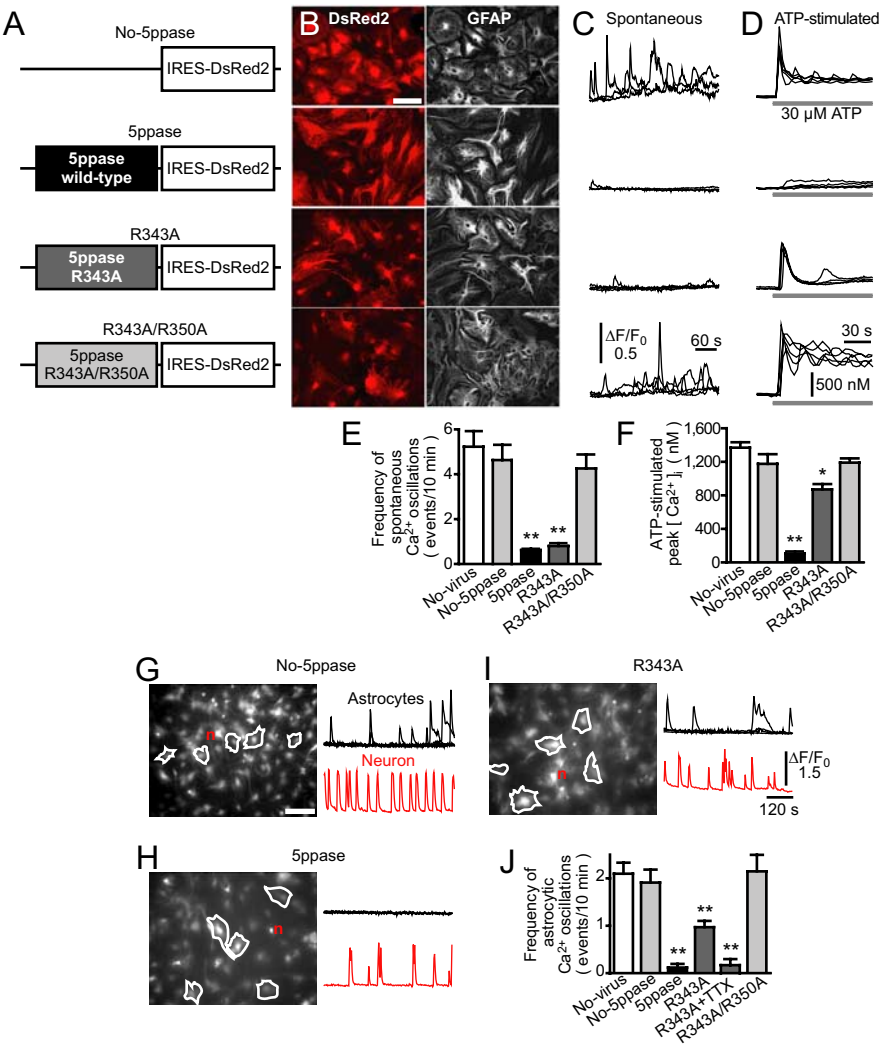

Figure 2. Establishment of Ca^{2+} signal-deficient astrocytes by retroviral transduction of 5ppase. ***A***, Constructs carried by retroviral vectors. cDNAs encoding wild-type 5ppase (5ppase) and its mutants (R343A and R343A/R350A) were transduced together with the infection marker DsRed2. ***B***, Representative images of DsRed2 fluorescence (left) and GFAP immunostaining (right) for retrovirus-infected astrocytes (No-5ppase, 5ppase, R343A, and R343A/R350A). Scale bar, 100 μm. ***C***, Spontaneous Ca^{2+} oscillations in astrocytes measured with fluo-4. Four representative traces of normalized fluorescence intensity ($\Delta F/F_0$) from each group of astrocytes were superimposed. ***D***, ATP-stimulated Ca^{2+} transients in astrocytes measured with fura-2. Five representative traces from each group of astrocytes were superimposed. ATP (30 μM) was applied during the time indicated by the bars under the traces. ***E***, ***F***, Summarized results of the frequency of spontaneous Ca^{2+} oscillations and peak $[Ca^{2+}]_i$ induced by ATP (mean + SEM; $n = 35–69$ and 13–27). *$p < 0.05$ and **$p < 0.01$ compared with No-virus (no-virus applied astrocytes), No-5ppase, and R343A/R350A using one-way ANOVA with Tukey's *post hoc* test. ***G–I***, Neurons cultured for 10–18 d on the monolayer of retrovirus-infected astrocytes (No-5ppase, 5ppase, or R343A). Representative Ca^{2+} signals measured with fluo-4 in astrocytes and a neuron (*n*) from each group (regions of interest are indicated in left images). Scale bar, 150 μm. ***J***, The frequency of Ca^{2+} transients in astrocytes cultured with neurons (mean + SEM; $n = 136–179$; $n = 28$ for R343A+TTX). **$p < 0.01$, compared with No-virus, No-5ppase, and R343A/R350A using one-way ANOVA with Tukey's *post hoc* test.

the Inverse Pericam2 construct. After culturing for at least 6 d, dissociated neurons were plated on the Inverse Pericam2-expressing astrocytes, and then, 12–18 d later, DsRedExpress or TurboRFP (Evrogen, Moscow, Russia) was transduced by lentiviruses or transient transfection, respectively, to visualize neurons. Images were acquired in the culture medium (see above) without phenol red using the Olympus IX81-ZDC system (~520 nm; emission, ~590 nm for DsRedExpress and TurboRFP) at 37°C, in 5% CO_2. The expression levels of these fluorescent proteins in Inverse Pericam2-expressing astrocytes were negligibly low. The fluorescence images of these cocultures were acquired every 6–12 s using the Olympus IX81-ZDC system at 37°C in 5% CO_2.

All images were analyzed using MetaMorph 6 software (Molecular Devices) or IPLab 3.2 software (Scanalytics, Fairfax, VA).

Immunocytochemistry. Cocultures or astrocyte monolayers were fixed by PBS containing 4% formaldehyde for 10 min at RT and then permeabilized by PBS containing 0.2% Triton X-100 (Sigma) for 5 min at RT. After blocking with PBS containing 10% BSA for 30 min at RT, these were incubated with primary antibodies in PBS containing 3% BSA for 1 h at RT or 16 h at 4°C. For primary antibodies, the following were used: mouse anti-GFAP (1:1000; Chemicon, Temecula, CA), rabbit anti-GFAP (1:200; Sigma), mouse anti-microtubule-associated protein 2 (MAP2) (1:1000; Chemicon), mouse anti-class III β-tubulin (1:1000; Covance, Berkeley, CA), mouse anti-N-cadherin (1:1000; BD Bioscience, San Jose, CA), rabbit anti-laminin (1:1000; the permeabilization step was omitted to observe extracellular laminin; Biomedical Technologies, Stoughton, MA), rabbit anti-fibronectin (1:1000; Dako Cytomation, Carpenteria, CA), rabbit anti-neural cell adhesion molecule (NCAM) (1:1000; Chemicon), rabbit anti-chondroitin sulfate proteoglycan (CSPG) (CS56, 1:1000; Sigma), and mouse anti-tenascin (a ready-to-use product was used without dilution; Lab Vision, Fremont, CA). The cells were then incubated with Alexa (488, 546, and 647) fluor-labeled goat anti-mouse or rabbit IgG (Invitrogen) as the secondary antibody (1:2000–5000) for 1 h at RT in PBS. The fluorescence images were acquired using the Olympus IX81-ZDC system with appropriate filter set for excitation (Alexa 488: excitation, ~480 nm; emission, <510 nm; Alexa 546: excitation, ~520 nm; emission, ~590 nm; Alexa 647: excitation, ~640 nm; emission, <650 nm) and emission in PBS at RT. The total dendritic length per immunostained neuron was analyzed using a neurite outgrowth plug-in of MetaMorph 6 software. For determining relative expression levels of growth-regulating proteins in 5ppase-expressing or pharmacological inhibitor-treated astrocytes, immunofluorescence intensity of each transduced (DsRed2 positive) or inhibitor-treated astrocyte was normalized by the mean immunofluorescence intensity of uninfected (DsRed2 negative) or no-inhibitor-applied astrocytes, respectively. Each region of interest of astrocyte was defined by the images of GFAP immunostaining.

Western blotting. Monolayers of astrocytes expressing 5ppases (infection rate, >80%) were lysed in SDS-containing buffer and boiled before immunoblot analysis. After electrophoresis, separated products were transferred to polyvinylidene difluoride membrane (Bio-Rad, Hercules, CA) and probed by incubation with antibodies against N-cadherin (1:1000; BD Bioscience) or glyceraldehyde-3-phosphate dehydrogenase (GAPDH) (1:2500; Chemicon) for 1 h at RT. Blots were then incubated with HRP-conjugated goat anti-rabbit or mouse antibody (MBL, Aichi, Japan) for 1 h at RT. Immunoreactive bands were detected using the Western Lighting system (PerkinElmer, Boston, MA).

Real-time PCR analysis. Total RNA purified from astrocytes using an RNeasy kit (Qiagen, Hilden, Germany) was amplified with superscript (Invitrogen) to obtain cDNAs. The level of N-cadherin mRNA was determined by real-time PCR analysis using TaqMan(R) Gene Expression Assays [primer

and probe set (Rn00580099_m1) for rat cdh2 (NM_031333.1)] with an ABI PRISM 7900 HT (Applied Biosystems, Foster City, CA). Relative mRNA level compared with the level of GAPDH (TaqMan Rodent GAPDH control Reagents VIC Probe; Applied Biosystems) mRNA was calculated by comparative Ct method.

Results

Neurite growth on thapsigargin-treated astrocytes

To study whether astrocytic Ca^{2+} signals are involved in neurite growth, we first examined the growth of dissociated rat hippocampal neurons that were cultured on monolayers of astrocytes, the Ca^{2+} signals of which were pharmacologically inhibited. Most of the inhibitors of astrocytic Ca^{2+} signals (Aguado et al., 2002; Nett et al., 2002; Koizumi et al., 2003) are not suitable for such experiments, because they also affect neuronal Ca^{2+} signals that are essential for neurite growth (Miller and Kaplan, 2003; Gomez and Zheng, 2006). To circumvent this problem, we used an irreversible inhibitor of sarco/endoplasmic reticulum Ca^{2+}-ATPase, thapsigargin, to deplete stored Ca^{2+} in the endoplasmic reticulum of astrocytes. Control astrocytes showed spontaneous Ca^{2+} oscillations, as reported previously (Parri et al., 2001; Koizumi et al., 2003). Thapsigargin treatment inhibited spontaneous Ca^{2+} oscillations for over 3 d even after the drug was washed away (Fig. 1*A*). Thus, fresh neurons were plated over thapsigargin-pretreated astrocytes in the absence of the drug and were cultured for 36 h. The analysis of the total neurite length of immunostained neurons showed that neurite growth was markedly suppressed when neurons were cultured on the drug-pretreated astrocytes (Fig. 1*B*,*C*) [mean total neurite length per cell was 20.85 ± 4.31 nm (mean ± SEM; $n = 111$) on thapsigargin-pretreated astrocytes, whereas 54.30 ± 5.03 nm ($n = 133$) on control astrocytes ($p < 0.01$; Mann–Whitney U test)], supporting the hypothesis that astrocytic Ca^{2+} signals are involved in the regulation of neurite growth.

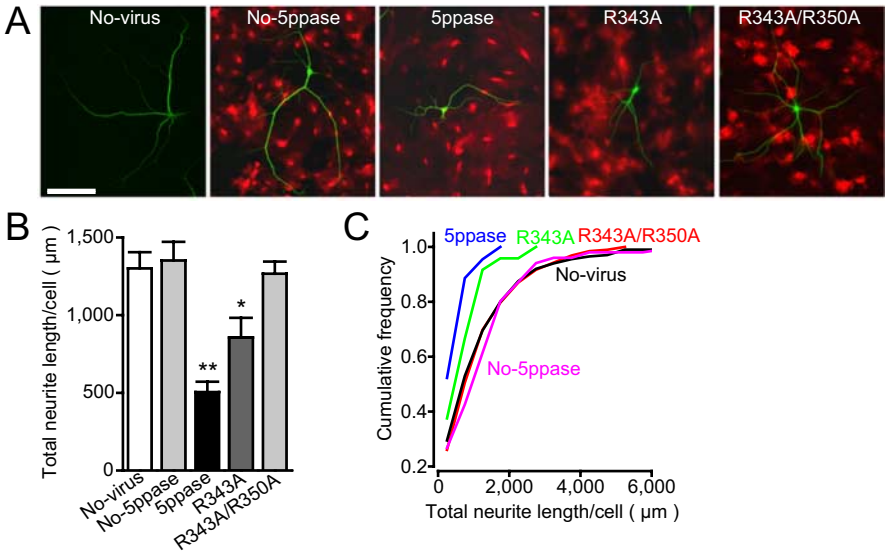

Figure 3. Suppression of dendritic growth on Ca^{2+} signal-deficient astrocytes. ***A***, Representative images of dendritic processes (MAP2-immunostaining; green) in neurons cultured for 21 d on the astrocyte monolayers infected with retrovirus encoding the construct of No-5ppase, wild-type 5ppase, R343A, or R343A/R350A (fluorescence image of DsRed2; red). The astrocytes that were not infected with viruses were also used as the control (No-virus). Scale bar, 150 μm. ***B***, ***C***, Total dendritic lengths per neuron are shown by bar graphs (mean + SEM) and cumulative histograms ($n = 44–101$). *$p < 0.05$ and **$p < 0.01$, compared with No-virus, No-5ppase, and R343A/R350A using one-way ANOVA with Tukey's *post hoc* test. The statistical significance ($p < 0.001$) between 5ppase (wild-type and R343A) and controls (No-virus, No-5ppase, and R343A/R350A) in cumulative histograms was confirmed by the Kolmogorov–Smirnov test.

Establishment of Ca^{2+} signal-deficient astrocytes by extrinsic IP_3 5-phosphatase

Culturing for >4 d is required to examine whether astrocytic Ca^{2+} signals contribute to the long-term growth of dendrites and axons (Dotti et al., 1988). The thapsigargin-induced suppression of astrocytic Ca^{2+} signals is not suitable for such long-term experiments, because the drug treatment eventually disrupts protein synthesis (Mattson et al., 2000). Thus, we used extrinsically expressed 5ppase to inhibit IP_3 signaling (Hirose et al., 1999; Okubo et al., 2001, 2004; Furutani et al., 2006; Suh et al., 2006), which has an essential role in astrocytic Ca^{2+} signals (Verkhratsky et al., 1998; Aguado et al., 2002; Nett et al., 2002; Koizumi et al., 2003). We generated a retrovirus harboring the construct of 5ppase and an infection marker, DsRed2, downstream of an IRES (Fig. 2*A*, 5ppase). We also generated retroviruses transducing only IRES-DsRed2 (No-5ppase) or one of the two mutants of 5ppase with a weak (R343A) and virtually no (R343A/R350A) phosphatase activity (Communi et al., 1996; Okubo et al., 2001). The latter, in which two arginine residues in the active site of the enzyme are replaced with alanine, was used as a phosphatase-negative control. Using these retroviruses, we obtained 5ppase-transduced astrocytes with a high infection rate (>90%) (Fig. 2*B*). These cells, which remain viable over 2 months in culture, can be replated >10 times (astrocytes replated five to seven times were used in the present experiments) and formed astrocytic monolayers normally, suggesting cellular Ca^{2+} homeostasis required for cellular housekeeping is retained.

We then evaluated the effect of wild-type and mutant 5ppases on astrocytic Ca^{2+} signals. Astrocytes expressing DsRed2 only or R343A/R350A mutant 5ppase showed spontaneous Ca^{2+} oscillations at nearly the same frequency as that in astrocytes without virus infection (No-virus) (Fig. 2*C*,*E*). These astrocytes also responded to bath-applied ATP with robust Ca^{2+} transients as described previously (Nett et al., 2002; Koizumi et al., 2003) (Fig. 2*D*,*F*). In contrast, virtually no spontaneous or ATP-stimulated Ca^{2+} signals were observed in astrocytes expressing wild-type 5ppase. There was no significant change in the resting intracellular Ca^{2+} concentration ($[Ca^{2+}]_i$) among each group. Notably, astrocytes expressing R343A mutant 5ppase showed almost no spontaneous Ca^{2+} oscillations, whereas they responded to ATP with a considerable increase in $[Ca^{2+}]_i$. Therefore, the phosphatase activity of the R343A mutant is sufficient to decrease the baseline IP_3 concentration during spontaneous Ca^{2+} oscillations but is insufficient to suppress agonist-evoked IP_3 signaling.

We next examined the effect of 5ppase on astrocytic Ca^{2+} signals in neuron-astrocyte cocultures. Neurons generated spontaneous bursting activities in all cocultures (Fig. 2*G–I*, red traces), making it possible that the astrocytes in these cocultures produce Ca^{2+} signals in response to neurotrans-

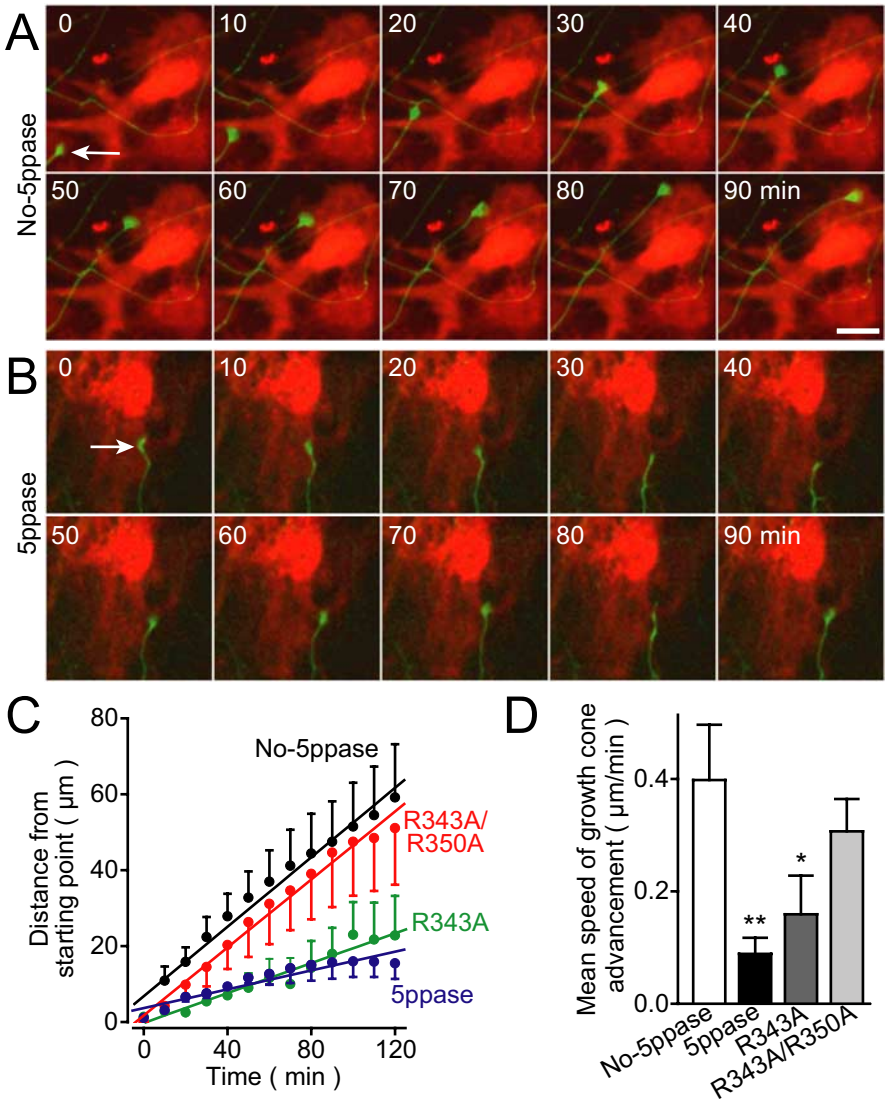

Figure 4. Suppression of growth cone advancement on Ca^{2+} signal-deficient astrocytes. ***A***, ***B***, Time-lapse images of growth cones (arrows) of GFP-expressing neurons (green) on astrocytes (red) transduced with No-5ppase (***A***) or wild-type 5ppase (***B***). Scale bar, 20 μm. See supplemental Movies 1 and 2 (available at www.jneurosci.org as supplemental material). ***C***, ***D***, Summarized time courses (***C***) and mean speed of growth cone advancement (***D***) in each group of astrocytes (No-5ppase, 5ppase, R343A, and R343A/R350A; mean ± SEM; $n = 17–18$). *$p < 0.05$ and **$p < 0.01$, compared with No-5ppase using one-way ANOVA with Tukey's *post hoc* test. Neurons at 10–18 d *in vitro* were imaged.

mitters and/or neurotrophins released from neurons in an activity-dependent manner (Verkhratsky et al., 1998; Aguado et al., 2002; Nett et al., 2002; Koizumi et al., 2003; Rose et al., 2003). Control astrocytes expressing DsRed2 only (No-5ppase) showed Ca^{2+} oscillations at a lower frequency than astrocytic monocultures (Fig. 2, compare *C* and *G*) probably because of a putative inhibitory effect of neurons on astrocytic Ca^{2+} signals (Koizumi et al., 2003). In contrast, astrocytes expressing wild-type 5ppase showed no Ca^{2+} oscillations (Fig. 2*H*,*J*). Interestingly, astrocytes expressing R343A mutant 5ppase showed Ca^{2+} oscillations, although their frequency was approximately one-half of that in control astrocytes (Fig. 2*I*,*J*). The residual Ca^{2+} signals in astrocytes expressing R343A mutant 5ppase may be neuronally evoked Ca^{2+} oscillations, because R343A mutant 5ppase is not able to suppress evoked Ca^{2+} signals as shown by the results of astrocytic monocultures (Fig. 2*D*,*F*). Indeed, the residual Ca^{2+} signals were abolished by the blockade of neuronal firing with tetrodotoxin (Fig. 2*J*, R343A+TTX).

Therefore, we established a method to generate astrocytes in which their Ca^{2+} signals are completely inhibited by wild-type 5ppase and those in which spontaneous Ca^{2+} oscillations are selectively suppressed by R343A mutant 5ppase. Together with the absence of noticeable cytotoxicity, this method is useful for clarifying the contribution of astrocytic Ca^{2+} signals to neuronal development.

Suppression of dendritic growth and growth cone advancement on Ca^{2+} signal-deficient astrocytes

Using these Ca^{2+} signal-deficient astrocytes, we examined the contribution of astrocytic Ca^{2+} signals to the growth of dendrites and axons. We cultured hippocampal neurons for 3 weeks on a monolayer of astrocytes expressing wild-type or mutant 5ppase. We first analyzed their dendritic length by immunostaining a dendrite-specific protein, MAP2. The total dendritic length of neurons cultured on astrocytes expressing either wild-type or R343A mutant 5ppase was significantly shorter than that of neurons cultured on control astrocytes (No-virus, No-5ppasse, and R343A/R350A) (Fig. 3*A–C*), indicating that astrocytic spontaneous Ca^{2+} oscillations significantly contribute to dendritic growth.

We next analyzed axonal growth on Ca^{2+} signal-deficient astrocytes. Here, we monitored the movement of growth cones, the palm-like tips of extending axons (supplemental Fig. 1, available at www.jneurosci.org as supplemental material), by time-lapse imaging. On control astrocytes, the growth cones of GFP-expressing neurons were highly motile and showed successive advancement at a speed of 0.4 μm/min on average (Fig. 4*A*,*C*, *D*, No-5ppase) (supplemental Movie 1, available at www.jneurosci.org as supplemental material). On 5ppase-expressing astrocytes, in contrast, growth cones were less motile and frequently showed transient retractive movements that were sometimes followed by growth cone collapse (Fig. 4*B*) (supplemental Movie 2, available at www.jneurosci.org as supplemental material). The average speed of growth cone advancement on the astrocytes expressing wild-type 5ppase was significantly lower than that on control astrocytes expressing DsRed2 only or R343A/R350A mutant 5ppase (Fig. 4*C*,*D*). Notably, the velocity of growth cone advancement was also significantly decreased on R343A mutant 5ppase-expressing astrocytes, in which spontaneous Ca^{2+} oscillations but not neuronally evoked Ca^{2+} transients were inhibited (Fig. 4*C*,*D*). These results indicate that astrocytic Ca^{2+} signals, in particular spontaneous Ca^{2+} oscillations, are indispensable for axonal growth.

Requirement of direct contact between neurons and astrocytes for Ca^{2+} signal-dependent regulation of growth cone movement

Astrocytes regulate neurite growth via diffusible cues as well as via nondiffusible membrane-bound proteins and ECM molecules (Neugebauer et al., 1988; Tomaselli et al., 1988; Muller et al., 1995; Crone and Lee, 2002). The former molecules exert their effects from a distance, whereas the latter molecules function in the immediate vicinity of astrocytes. To clarify whether diffusible or nondiffusible molecules are involved in the suppression of growth cone advancement on Ca^{2+} signal-deficient astrocytes, we prepared cultures in which normal and Ca^{2+} signal-deficient astrocytes were randomly distributed by decreasing the virus infection probability. Then, we compared the growth cone advancement on an uninfected astrocyte with that on a neighboring 5ppase-expressing astrocyte (Fig. 5*A*). The growth cone shown in time-lapse images (Fig. 5*B*) (supplemental Movie 3, available at www.jneurosci.org as supplemental material) advanced steadily on the uninfected astrocyte, but it almost halted its movement after its contact with the 5ppase-expressing astrocyte. Figure 5*C* shows the trajectory of the center of growth cone imaged every 10 min during the 4 h observation period. When the growth cone was advancing on the uninfected astrocyte, the trajectory was almost straight. However, it was bent many times after its contact with the 5ppase-expressing astrocyte, indicating that the advancement was suppressed immediately after the contact with the Ca^{2+} signal-deficient astrocyte. The growth cone sometimes showed a transient retractive movement accompanied by growth cone collapse (supplemental Movie 3, available at www.jneurosci.org as supplemental material). The average speed of advancement decreased by approximately sevenfold after the contact with the 5ppase-expressing astrocyte (Fig. 5*D*). Similar results were obtained in other samples and in experiments using astrocytes expressing R343A mutant 5ppase (Fig. 5*E*). These results suggest that nondiffusible factors in the immediate vicinity of astrocytes are involved in the regulation of growth cone advancement.

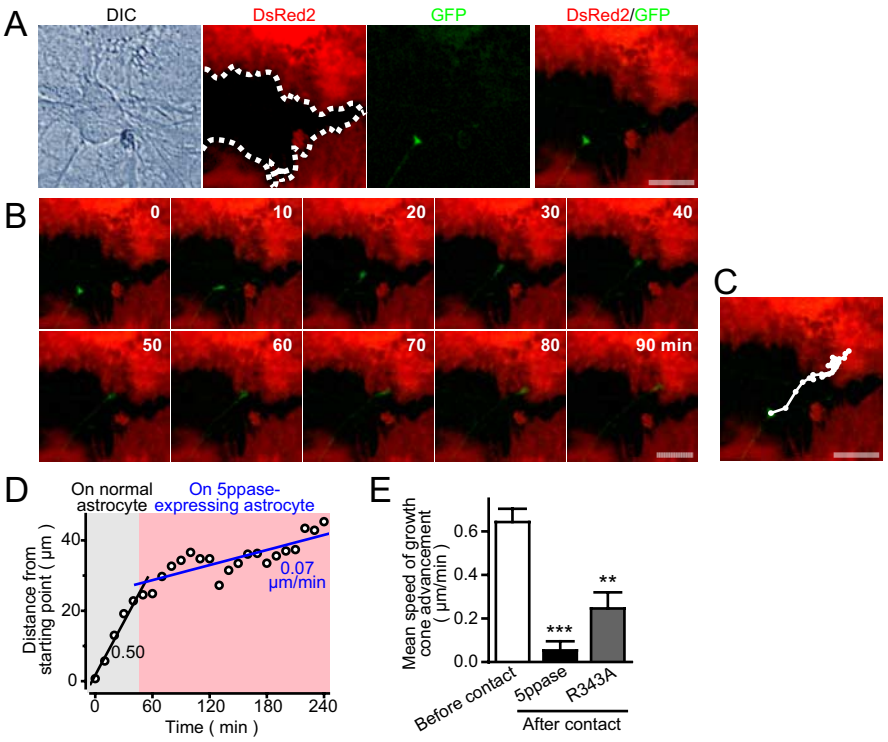

Figure 5. Suppression of growth cone advancement depends on contact with Ca^{2+} signal-deficient astrocytes. ***A***, The boundary of between astrocytes with (red) and without (black) wild-type 5ppase expression is shown by the dotted line. Uninfected cells are confirmed by the DIC image. Infection rate was lowered so that 30% of astrocytes remain uninfected with 5ppase-transducing retroviruses. The growth cone of a GFP-expressing neuron on an uninfected astrocyte adjacent to 5ppase-expressing astrocytes is shown. ***B***, ***C***, Time-lapse images of growth cone movement and the trajectory of the center of growth cone. See supplemental Movie 3 (available at www.jneurosci.org as supplemental material). ***D***, Plot of growth cone advancement against time. Note that the speed of growth cone advancement decreased immediately after the contact with 5ppase-expressing astrocyte. ***E***, Mean speed of growth cone advancement before and after contact with 5ppase- or R343A-expressing astrocyte (mean + SEM; $n = 17$, 13, and 4 for before contact, 5ppase, and R343A, respectively). $^{**}p < 0.01$ and $^{***}p < 0.001$, with Student's *t* test (vs before contact). Scale bars, 20 μm.

Simultaneous imaging of astrocytic Ca^{2+} signals and growth cone advancement

The results thus far suggest that ongoing Ca^{2+} oscillations maintain the surface of astrocytes suitable for the growth of neurites. However, there remains an alternative possibility that the contact of growth cones with astrocytes induces an astrocytic IP_3-Ca^{2+} signal that activates an instantaneous mechanism on the astrocyte membrane to promote growth cone advancement, and that such IP_3-Ca^{2+} signal is suppressed by 5ppase. To test this possibility, we simultaneously imaged astrocytic Ca^{2+} signals and growth cone advancement and compared the Ca^{2+} signals before and after the growth cone contact. It takes a few hours for growth cones to move from an astrocyte to its neighbor cell. None of the small molecular Ca^{2+} indicators such as fura-2 was suitable for such a long-duration Ca^{2+} imaging because of their leakage from the cells. We therefore used a genetically encoded Ca^{2+} indicator, Inverse Pericam2 [a modified Inverse Pericam (Nagai et al., 2001; Ishii et al., 2006); see Materials and Methods] and expressed it in astrocytes using a lentiviral vector. Figure 6*A* shows the growth cone of a red fluorescence protein (RFP)-expressing neuron on an astrocyte expressing Inverse Pericam2. The growth cone traveled over two neighboring astrocytes in ~3 h (Fig. 6*B*). Although we were able to observe spontaneous Ca^{2+} oscillations in astrocytes with Inverse Pericam2, we did not find any obvious additional Ca^{2+} signals during the growth cone contact. Furthermore, the frequency and the amplitude of Ca^{2+} oscillations in these astrocytes did not change before, during, or after the contact with the growth cone (Fig. 6*C*). Similar results were obtained in 19 sets of growth cones and astrocytes (Fig. 6*D*), indicating that astrocytic Ca^{2+} signals are not affected by the contact of growth cones. Together with the results obtained using the astrocytes expressing R343A mutant 5ppase (Figs. 4, 5), these results indicate that ongoing spontaneous Ca^{2+} oscillations are critical for the maintenance of astrocytic function to promote growth cone advancement.

Reduced expression of N-cadherin in Ca^{2+} signal-deficient astrocytes

The above results indicate that membrane proteins and/or ECM molecules on the surface of astrocytes are likely involved in the

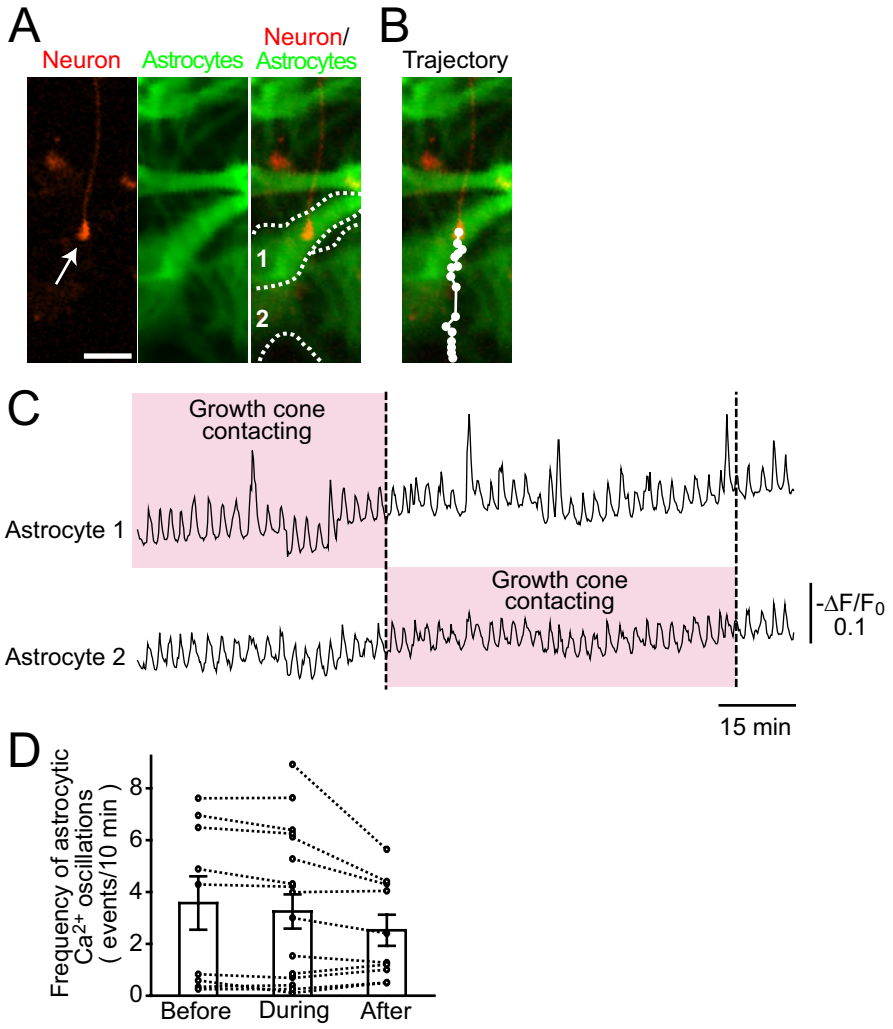

Figure 6. Simultaneous imaging of growth cone advancement and astrocytic Ca^{2+} signals. ***A***, The growth cone of an RFP-expressing neuron (red) and astrocytes expressing genetically encoded Ca^{2+} indicator, Inverse Pericam2 (green) are shown. The boundaries of two astrocytes (astrocytes 1 and 2) are indicated by the dotted lines. Scale bar, 20 μm. ***B***, The trajectory of growth cone advancement in 200 min. The growth cone moved from astrocyte 1 to astrocyte 2. ***C***, Ca^{2+} signals in astrocytes 1 and 2 during the movement of the growth cone ($-\Delta F/F_0$). The growth cone made contact with each astrocyte during the periods indicated by the pink boxes. No noticeable change in the frequency of astrocytic Ca^{2+} oscillations was observed during growth cone contact. ***D***, The results from 19 sets of growth cones and astrocytes were summarized. The mean frequency of Ca^{2+} signals in each astrocyte before, during, and after contact was plotted (circle and dotted line). Bar graphs show the mean ± SEM at each period.

Ca^{2+} oscillation-dependent regulation of neurite growth. As an initial step to understand the molecular basis of the astrocyte-dependent growth cone advancement, we examined whether there is any change in the expression of surface proteins of Ca^{2+} signal-deficient astrocytes. Astrocytes express N-cadherin, laminin, fibronectin, and NCAM to promote neurite growth (Neugebauer et al., 1988; Tomaselli et al., 1988; Muller et al., 1995). Conversely, both CSPGs and tenascin provided by astrocytes (Muller et al., 1995; Sandvig et al., 2004) inhibit neurite growth. Therefore, the downregulation of the former proteins or the upregulation of the latter proteins may account for the suppression of growth cone advancement on Ca^{2+} signal-deficient astrocytes. To examine these possibilities, we immunocytochemically analyzed the expression levels of these proteins in Ca^{2+} signal-deficient astrocytes. Interestingly, the expression level of N-cadherin was significantly lower in the astrocytes expressing wild-type or R343A mutant 5ppase than in uninfected cells, whereas astrocytes expressing R343A/R350A mutant 5ppase expressed the same level of N-cadherin as uninfected cells (Fig. 7*A*,*B*). In contrast, there were no significant changes in the expression level of other molecules (laminin, fibronectin, NCAM, CSPGs, and tenascin) in Ca^{2+} signal-deficient astrocytes (supplemental Fig. 2, available at www.jneurosci.org as supplemental material). Western blot and real-time PCR analysis also showed that the expression level of N-cadherin decreased in Ca^{2+} signal-deficient astrocytes (Fig. 7*C*,*D*).

It seems probable that the downregulation of N-cadherin is responsible for the neurite-growth suppression on Ca^{2+} signal-deficient astrocytes, because the role of N-cadherin as an enhancer of neurite growth has been reported (Neugebauer et al., 1988; Tomaselli et al., 1988; Williams et al., 1994; Muller et al., 1995). Therefore, we studied the functional significance of N-cadherin in the neurite growth in our experimental system and the causal relationship between decreased N-cadherin expression level and neurite-growth suppression on Ca^{2+} signal-deficient astrocytes. Indeed, we found that the speed of growth cone advancement on normal astrocytes significantly decreased in the presence of a function-blocking antibody to N-cadherin (Fig. 7*E*, left). No change in the astrocytic Ca^{2+} signals was observed in the presence of antibody (data not shown). Moreover, the deficiency of growth cone advancement on 5ppase-expressing astrocytes was rescued by extrinsic N-cadherin expression (Fig. 7*E*, right). These results suggest that spontaneous Ca^{2+} oscillations in astrocytes are involved in the maintenance of maintain N-cadherin expression to promote neurite growth.

Discussion

Intracellular Ca^{2+} signaling in astrocytes is currently studied with intensive interest as a possible mediator of the neuron-astrocyte communication. Although there is accumulating evidence that astrocytic Ca^{2+} signals are involved in the instantaneous modulation of synaptic transmission and neuronal firing patterns via the release of "gliotransmitters" (Koizumi et al., 2003; Zhang et al., 2003; Fellin et al., 2004), little has been known whether astrocytic Ca^{2+} signals are involved in the regulation of neuronal development, one of the important roles of astrocytes. The lack of methods to keep astrocytic Ca^{2+} signals suppressed for a long period seems to have prevented the clarification of this issue. In the present study, we overcame this difficulty by the stable expression of 5ppase, an IP_3-hydrolyzing enzyme, and its mutants to produce astrocytes in which Ca^{2+} signals were suppressed to various extents. Using these Ca^{2+} signal-deficient astrocytes, we found that ongoing spontaneous Ca^{2+} oscillations

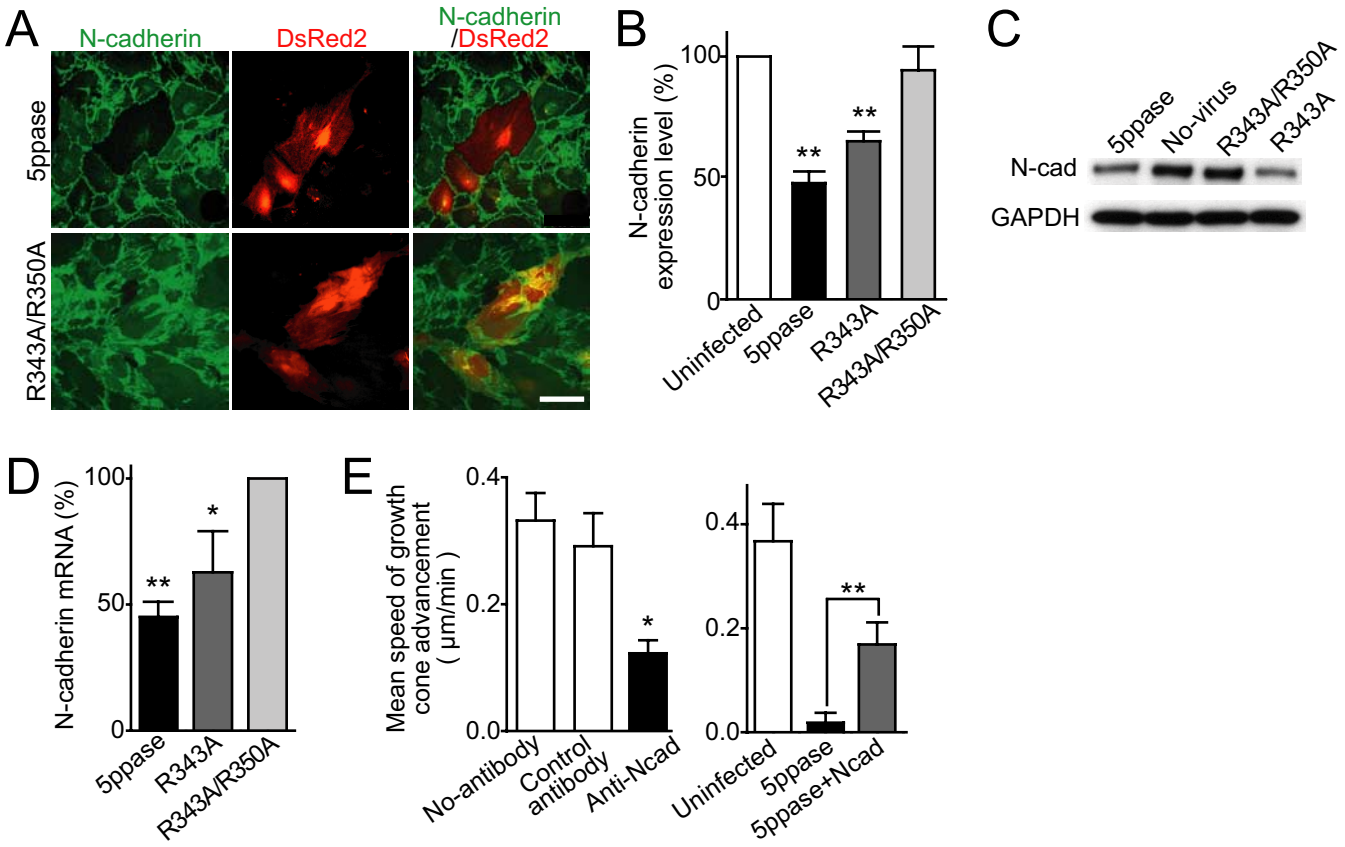

Figure 7. Decreased N-cadherin expression level in Ca^{2+} signal-deficient astrocytes. ***A***, Representative immunocytochemical images of N-cadherin (green) in control (R343A/R350A) and wild-type 5ppase-expressing astrocytes. Transduced astrocytes express DsRed2 (red). ***B***, N-cadherin immunofluorescence intensity of virus-infected astrocytes (5ppase, R343A, and R343A/R350A) normalized with that of uninfected astrocytes in the same culture (mean + SEM; $n = 21–35$). ***C***, Western blot analysis of N-cadherin (N-cad) expression level in virus-infected (5ppase, R343A, and R343A/R350A) and uninfected (No-virus) astrocytes. ***D***, N-cadherin mRNA level in astrocytes expressing 5ppase was quantified using real-time PCR analysis (mean + SEM; $n = 3–5$). Values were normalized by those in astrocytes expressing R343A/R350A mutant 5ppase. ***E***, Speed of growth cone advancement in the absence (No-antibody) or presence of a function-blocking antibody to N-cadherin (Anti-Ncad) or anti-Flag antibody (Control antibody) (left; mean + SEM; $n = 9–11$) and on uninfected, 5ppase-expressing, and [5ppase plus extrinsic N-cadherin]-expressing astrocytes (right; mean + SEM; $n = 5–10$). $*p < 0.05$, $**p < 0.01$, and N.S. (not significant; $p > 0.5$) with Student's *t* test in ***B***, ***D***, and ***E*** (vs uninfected for ***B*** and ***E***, vs R343A/R350A for ***D***). Scale bars, 100 μm.

are indispensable for astrocytes to promote neurite growth. The present study thus suggested a novel relationship between astrocytic Ca^{2+} signals and neuronal development.

Distinct role of spontaneous Ca^{2+} oscillations and neurotransmitter-evoked Ca^{2+} transients

In addition to spontaneous Ca^{2+} oscillations, astrocytes show different patterns of Ca^{2+} signals. It was shown that neurotransmitter-evoked Ca^{2+} transients (Koizumi et al., 2003; Zhang et al., 2003; Fellin et al., 2004) and spontaneous Ca^{2+} spikes with large amplitudes (Parri et al., 2001) induce the release of ATP and glutamate as the gliotransmitters, which in turn modulate synaptic transmission and the firing pattern of adjacent neurons. We found that R343A mutant 5ppase, which suppresses spontaneous Ca^{2+} oscillations but does not abolish neuronally evoked Ca^{2+} signals, was able to inhibit dendritic growth and growth cone advancement. This finding suggests that astrocytic functions are differentially regulated by the pattern of intracellular Ca^{2+} signals. Ca^{2+} signals with large amplitudes and short durations, such as neuronally evoked Ca^{2+} transients, may modulate neuronal functions by releasing gliotransmitters. In contrast, long-lasting spontaneous Ca^{2+} oscillations with low amplitudes may be mainly involved in neuronal development.

Mechanism for the regulation of neurite growth by spontaneous Ca^{2+} oscillation in astrocytes

Our results suggest that N-cadherin is one of the key molecules downstream of spontaneous Ca^{2+} oscillations in astrocytes to promote neurite growth. This notion is consistent with the role of N-cadherin in growth cone advancement (Neugebauer et al., 1988; Tomaselli et al., 1988; Williams et al., 1994; Muller et al., 1995). Although Ca^{2+} signals regulate the expression and functions of various proteins (Berridge et al., 2000), 5ppase-mediated suppression of Ca^{2+} oscillations in astrocytes did not induce nonspecific changes in protein expression. It decreased N-cadherin expression level without significant changes in the expression of five other growth-regulating proteins (Fig. 7*A–D*) (supplemental Fig. 2, available at www.jneurosci.org as supplemental material). This suggests that astrocytic Ca^{2+} oscillations regulate the expression of a limited number of specific proteins. The specificity may be explained by the temporal patterns of Ca^{2+} signals, which are critical for the encoding of downstream signaling mechanisms (Dolmetsch et al., 1998; Tomida et al., 2003). The evaluation of the signaling pathway downstream of Ca^{2+} oscillations in conjunction with N-cadherin transcription is currently being addressed.

Applications of 5ppase as an inhibitor of glial Ca^{2+} signals

Numerous receptors and downstream pathways mediate the formation of Ca^{2+} signals in astrocytes. Therefore, it has been difficult to completely silence astrocytic Ca^{2+} signals using pharmacological inhibitors. Furthermore, the application of the pharmacological inhibitors to neuron–astrocyte cocultures would also inhibit Ca^{2+} signals in neurons. Therefore, there has been no efficient method for the specific inhibition of Ca^{2+} signals in glial cells. The use of 5ppase is an efficient and specific method to chronically abolish astrocytic Ca^{2+} signals without detectable cytotoxicity even in a long-term culture. Moreover, mutant 5ppases that have submaximal phosphatase activity enable us to titrate IP_3 signaling to evaluate the significance of spontaneous Ca^{2+} oscillations of astrocytes.

The frequency of spontaneous astrocytic Ca^{2+} oscillations in the early postnatal ventrobasal thalamus gradually decreases with age, and the period when spontaneous Ca^{2+} oscillations are frequently observed corresponds to the period when axon and dendrites actively grow to form thalamocortical circuits (Parri et al., 2001). Moreover, radial glia, which is an astrocyte precursor cell, shows spontaneous Ca^{2+} oscillations and Ca^{2+} waves in a developing neocortex. It has been shown that these Ca^{2+} signals promote neuronal proliferation during neocortical development (Weissman et al., 2004). In injury sites of adult CNS, astrocytes turn into reactive astrocytes that inhibit neuronal growth and suppress axonal regeneration (Powell et al., 1997; Pekny and Nilsson, 2005). Notably, it was shown that reactive astrocytes do not generate spontaneous Ca^{2+} oscillations (Aguado et al., 2002). These findings suggest that spontaneous Ca^{2+} signaling in astrocytes as well as radial glial cells is important for neuronal development and regeneration. Using viral vectors or transgenic animals, these possibilities can now be addressed by applying the 5ppase method *in vivo*. Moreover, genome-wide screening in which wild-type and Ca^{2+} signal-deficient astrocytes are compared may allow us to identify novel molecules and pathways that regulate neuronal development and regeneration.

In conclusion, we clarified a new form of neuron–glia interaction using the 5ppase method. This method will provide deeper insights into the function of astrocytic Ca^{2+} signals.

References

Aguado F, Espinosa-Parrilla JF, Carmona MA, Soriano E (2002) Neuronal activity regulates correlated network properties of spontaneous calcium transients in astrocytes *in situ*. J Neurosci 22:9430–9444.

Araujo SJ, Tear G (2003) Axon guidance mechanisms and molecules: lessons from invertebrates. Nat Rev Neurosci 4:910–922.

Bahr M, Przyrembel C, Bastmeyer M (1995) Astrocytes from adult rat optic nerves are nonpermissive for regenerating retinal ganglion cell axons. Exp Neurol 131:211–220.

Berridge MJ, Lipp P, Bootman MD (2000) The versatility and universality of calcium signalling. Nat Rev Mol Cell Biol 1:11–21.

Communi D, Lecocq R, Erneux C (1996) Arginine 343 and 350 are two active residues involved in substrate binding by human Type I D-myo-inositol 1,4,5,-trisphosphate 5-phosphatase. J Biol Chem 271:11676–11683.

Crone SA, Lee KF (2002) The bound leading the bound: target-derived receptors act as guidance cues. Neuron 36:333–335.

Dolmetsch RE, Xu K, Lewis RS (1998) Calcium oscillations increase the efficiency and specificity of gene expression. Nature 392:933–936.

Dotti CG, Sullivan CA, Banker GA (1988) The establishment of polarity by hippocampal neurons in culture. J Neurosci 8:1454–1468.

Fellin T, Pascual O, Gobbo S, Pozzan T, Haydon PG, Carmignoto G (2004) Neuronal synchrony mediated by astrocytic glutamate through activation of extrasynaptic NMDA receptors. Neuron 43:729–743.

Furutani K, Okubo Y, Kakizawa S, Iino M (2006) Postsynaptic inositol 1,4,5-trisphosphate signaling maintains presynaptic function of parallel fiber-Purkinje cell synapses via BDNF. Proc Natl Acad Sci USA 103:8528–8533.

Gomez TM, Zheng JQ (2006) The molecular basis for calcium-dependent axon pathfinding. Nat Rev Neurosci 7:115–125.

Goslin K, Asmussen H, Banker G (1998) Rat hippocampal neurons in low-density culture. In: Culturing nerve cells, Ed 2. London: A Bradford Book.

Hama H, Hara C, Yamaguchi K, Miyawaki A (2004) PKC signaling mediates global enhancement of excitatory synaptogenesis in neurons triggered by local contact with astrocytes. Neuron 41:405–415.

Hirase H, Qian L, Bartho P, Buzsaki G (2004) Calcium dynamics of cortical astrocytic networks in vivo. PLoS Biol 2:E96.

Hirose K, Kadowaki S, Tanabe M, Takeshima H, Iino M (1999) Spatiotemporal dynamics of inositol 1,4,5-trisphosphate that underlies complex Ca^{2+} mobilization patterns. Science 284:1527–1530.

Ishii K, Hirose K, Iino M (2006) Ca^{2+} shuttling between endoplasmic reticulum and mitochondria underlying Ca^{2+} oscillations. EMBO Rep 7:390–396.

Koizumi S, Fujishita K, Tsuda M, Shigemoto-Mogami Y, Inoue K (2003) Dynamic inhibition of excitatory synaptic transmission by astrocyte-derived ATP in hippocampal cultures. Proc Natl Acad Sci USA 100:11023–11028.

Laxminarayan KM, Chan BK, Tetaz T, Bird PI, Mitchell CA (1994) Characterization of a cDNA encoding the 43-kDa membrane-associated inositol-polyphosphate 5-phosphatase. J Biol Chem 269:17305–17310.

Lois C, Hong EJ, Pease S, Brown EJ, Baltimore D (2002) Germline transmission and tissue-specific expression of transgenes delivered by lentiviral vectors. Science 295:868–872.

Mattson MP, LaFerla FM, Chan SL, Leissring MA, Shepel PN, Geiger JD (2000) Calcium signaling in the ER: its role in neuronal plasticity and neurodegenerative disorders. Trends Neurosci 23:222–229.

Miller FD, Kaplan DR (2003) Signaling mechanisms underlying dendrite formation. Curr Opin Neurobiol 13:391–398.

Miyakawa T, Mizushima A, Hirose K, Yamazawa T, Bezprozvanny I, Kurosaki T, Iino M (2001) Ca^{2+}-sensor region of IP_3 receptor controls intracellular Ca^{2+} signaling. EMBO J 20:1674–1680.

Muller HW, Junghans U, Kappler J (1995) Astroglial neurotrophic and neurite-promoting factors. Pharmacol Ther 65:1–18.

Nagai T, Sawano A, Park ES, Miyawaki A (2001) Circularly permuted green fluorescent proteins engineered to sense Ca^{2+}. Proc Natl Acad Sci USA 98:3197–3202.

Nett WJ, Oloff SH, McCarthy KD (2002) Hippocampal astrocytes in situ exhibit calcium oscillations that occur independent of neuronal activity. J Neurophysiol 87:528–537.

Neugebauer KM, Tomaselli KJ, Lilien J, Reichardt LF (1988) N-cadherin, NCAM, and integrins promote retinal neurite outgrowth on astrocytes in vitro. J Cell Biol 107:1177–1187.

Okubo Y, Kakizawa S, Hirose K, Iino M (2001) Visualization of IP_3 dynamics reveals a novel AMPA receptor-triggered IP_3 production pathway mediated by voltage-dependent Ca^{2+} influx in Purkinje cells. Neuron 32:113–122.

Okubo Y, Kakizawa S, Hirose K, Iino M (2004) Cross talk between metabotropic and ionotropic glutamate receptor-mediated signaling in parallel fiber-induced inositol 1,4,5-trisphosphate production in cerebellar Purkinje cells. J Neurosci 24:9513–9520.

Parri HR, Gould TM, Crunelli V (2001) Spontaneous astrocytic Ca^{2+} oscillations in situ drive NMDAR-mediated neuronal excitation. Nat Neurosci 4:803–812.

Pekny M, Nilsson M (2005) Astrocyte activation and reactive gliosis. Glia 50:427–434.

Powell EM, Meiners S, DiProspero NA, Geller HM (1997) Mechanisms of astrocyte-directed neurite guidance. Cell Tissue Res 290:385–393.

Rose CR, Blum R, Pichler B, Lepier A, Kafitz KW, Konnerth A (2003) Truncated TrkB-T1 mediates neurotrophin-evoked calcium signalling in glia cells. Nature 426:74–78.

Sandvig A, Berry M, Barrett LB, Butt A, Logan A (2004) Myelin-, reactive glia-, and scar-derived CNS axon growth inhibitors: expression, receptor signaling, and correlation with axon regeneration. Glia 46:225–251.

Silver J, Miller JH (2004) Regeneration beyond the glial scar. Nat Rev Neurosci 5:146–156.

Suh BC, Inoue T, Meyer T, Hille B (2006) Rapid chemically induced changes of $PtdIns(4,5)P_2$ gate KCNQ ion channels. Science 314:1454–1457.

Teng J, Rai T, Tanaka Y, Takei Y, Nakata T, Hirasawa M, Kulkarni AB, Hirokawa N (2005) The KIF3 motor transports N-cadherin and organizes the developing neuroepithelium. Nat Cell Biol 7:474–482.

Tomaselli KJ, Neugebauer KM, Bixby JL, Lilien J, Reichardt LF (1988) N-cadherin and integrins: two receptor systems that mediate neuronal process outgrowth on astrocyte surfaces. Neuron 1:33–43.

Tomida T, Hirose K, Takizawa A, Shibasaki F, Iino M (2003) NFAT functions as a working memory of Ca^{2+} signals in decoding Ca^{2+} oscillation. EMBO J 22:3825–3832.

Ullian EM, Sapperstein SK, Christopherson KS, Barres BA (2001) Control of synapse number by glia. Science 291:657–661.

Verkhratsky A, Orkand RK, Kettenmann H (1998) Glial calcium: homeostasis and signaling function. Physiol Rev 78:99–141.

Wang X, Lou N, Xu Q, Tian GF, Peng WG, Han X, Kang J, Takano T, Nedergaard M (2006) Astrocytic Ca^{2+} signaling evoked by sensory stimulation in vivo. Nat Neurosci 9:816–823.

Weissman TA, Riquelme PA, Ivic L, Flint AC, Kriegstein AR (2004) Calcium waves propagate through radial glial cells and modulate proliferation in the developing neocortex. Neuron 43:647–661.

Williams EJ, Furness J, Walsh FS, Doherty P (1994) Activation of the FGF receptor underlies neurite outgrowth stimulated by L1, N-CAM, and N-cadherin. Neuron 13:583–594.

Zhang JM, Wang HK, Ye CQ, Ge W, Chen Y, Jiang ZL, Wu CP, Poo MM, Duan S (2003) ATP released by astrocytes mediates glutamatergic activity-dependent heterosynaptic suppression. Neuron 40:971–982.